Residual internal stress in partially crystallized photothermorefractive glass: Evaluation by nuclear magnetic resonance spectroscopy and first principles calculations

J. W. Zwanziger[a] and U. Werner-Zwanziger
Department of Chemistry, Dalhousie University, Halifax, Nova Scotia B3H 4J3, Canada and Institute for Research in Materials, Dalhousie University, Halifax, Nova Scotia B3H 4J3, Canada

E. D. Zanotto
Vitreous Materials Laboratory, Department of Materials Engineering, Federal University of São Carlos, 13565-905 São Carlos, São Paulo, Brazil

E. Rotari, L. N. Glebova, and L. B. Glebov
College of Optics and Photonics, University of Central Florida, Orlando, Florida 32816

J. F. Schneider
Instituto de Física de São Carlos, Universidade de São Paulo, 13565-970 São Carlos, São Paulo, Brazil

(Received 26 September 2005; accepted 7 March 2006; published online 4 May 2006)

In some circumstances, the mechanical and optical properties of multiphase brittle materials strongly depend on the level of residual micromechanical stresses that arise upon cooling due to thermal and elastic mismatch between the constituent phases. Here we study the residual internal stress in a partially crystallized oxyfluoride glass, best known as photothermorefractive (PTR) glass. This material is composed of a glass matrix with embedded nanosize sodium fluoride (NaF) crystals. Using both the Selsing model and solid-state nuclear magnetic resonance in combination with first principles calculations we found that the crystals are under a tensile stress field of approximately 610–800 MPa. For this stress level the estimated critical crystal diameter for spontaneous cracking is about 2300–1900 nm, which greatly exceeds the observed diameters of 7–35 nm. Hence no spontaneous cracking is expected for the PTR glasses. First principles calculations indicate that the stress induced change of the refractive index of the NaF crystals is about −0.08%, which agrees with the observed refractive index changes. © *2006 American Institute of Physics*.
[DOI: 10.1063/1.2191731]

I. INTRODUCTION

The knowledge of internal residual stresses in multiphase materials has always been of interest from the standpoint of the mechanical behavior of multiphase materials. More recently, their possible effect on the optical properties of transparent glass ceramics reawakened the search for more precise ways to calculate and measure such stresses.

Glass ceramics are polycrystalline materials produced by controlled crystallization of glass having one or more crystal phases embedded in a glassy matrix. The ability to synthesize opaque or transparent articles of complex shapes, coupled with their lack of porosity and easy microstructural design make glass ceramics unique for both domestic and advanced applications, such as in microwave and optoelectronic devices,[1] surgical implants,[2] and large telescope mirrors.[3] Their mechanical, electrical, thermal, chemical, and optical, performances are major issues for such applications. Most of these properties strongly depend on some microstructural parameters and also on the level and type (tensile or compressive) of residual stresses around the precipitated crystals. These stresses appear on cooling partially crystallized specimens from the vicinity of the glass transition temperature T_g to room temperature, due to the thermal and elastic mismatch between the constituent phases.

While the overall effects of microstructure on the mechanical and optical properties are well established, much less is known on the effects of residual stresses.

Recently there has been increased activity on the study and development of transparent glass ceramics. One such material is a slightly crystallized oxyfluoride glass, known as photothermorefractive (PTR) glass, which is composed of a glass matrix with embedded nanosize NaF crystals. PTR glass is finding an increasing number of applications. PTR glass blanks with a diameter of up to 50 mm and homogeneity of refractive index better than 10^{-5} have been produced at the Center for Research and Education in Optics and Lasers (CREOL) at the University of Central Florida. This photosensitive glass enables the creation of diffracting optical components with the spectral and angular selectivity that are necessary for further development of PTR technology for high power laser beam control. PTR glasses are intended for use in high-accuracy (volume) holographic optical elements of laser and optoelectronic devices for optical target characterization, such as narrow band filters, attenuators, beam splitters, samplers, and multiplexers.

In this paper we use two independent methods to esti-

[a]Author to whom correspondence should be addressed; electronic mail: jzwanzig@dal.ca

mate the residual internal stresses. First, we use thermal and physical properties of the glass and crystal phases and the Selsing model.[4] We also use solid-state nuclear magnetic resonance (NMR) both to confirm the identification of the crystal phase and to estimate the residual stresses in the nanoparticles. The stress estimation is made by interpreting the observed shifts in the NMR spectra with accurate first principles calculations. The two methods of stress analysis are shown to be in quantitative agreement. NMR has been used previously to assess stress and strain qualitatively in composites[5–7] (specifically, multilayer films) and in amorphous films,[8] but in this study we determined quantitatively residual stress by NMR in a bulk composite. Finally, we estimate the stress induced change of the refractive index of the NaF crystals by first principles calculations and discuss the possible effect of these changes on the overall optical properties of PTR glass.

II. RESIDUAL STRESSES IN COMPOSITES

A. Theory

Selsing[4] developed a simple model of the stresses in a composite consisting of spherical particles embedded in an isotropic, elastic material. In this case the radial stress σ_r and the tangential stress σ_θ are given, respectively, by

$$\sigma_r = P(R/x)^3, \tag{1}$$

$$\sigma_\theta = -P/2(R/x)^3, \tag{2}$$

where P is the hydrostatic pressure on the inclusion, R is the particle radius, and x is the distance from the center of the inclusion. These equations are valid for $x \geqslant R$, that is, at the particle interface, where the stress is maximal, and outside, where it decreases as x^{-3}.

In glass ceramics the particles are expected to be in a state of considerable mechanical stress because of the kinetic arrest of the matrix at the glass transition coupled with the different elastic and thermal properties of the particles and the glass matrix. The hydrostatic thermal stress is predicted to be[4]

$$P = \frac{\Delta\alpha\Delta T}{(1+\nu_m)/2E_m + (1-2\nu_p)/E_p}. \tag{3}$$

The subscripts m and p refer to the matrix and particle, respectively. The mismatch in thermal expansivity is $\Delta\alpha = \alpha_p - \alpha_m$, with $\alpha = (\partial V/\partial T)/V$. ΔT is the difference between the temperature at which the glass matrix ceases to flow on cooling (roughly equal to the glass transition temperature T_g) and the ambient temperature. Finally, E and ν are, respectively, the elastic modulus and the Poisson ratio, again for the particles (subscript p) and the matrix (subscript m).

Equation (3) holds for particles dilute enough such that their stress fields do not overlap to any appreciable extent, which is expected to be the case when the particle volume fraction does not exceed 15%. In the present system, the embedded particles have a cubic structure and a volume fraction of less than 1%, so we expect the prediction of Eq. (3) to be valid.

Finally, we note that a critical diameter D_c for spontaneous cracking of the particle has been derived by Davidge and Green:[9]

$$D_c = \frac{8\gamma}{[(1+\nu_m)/2E_m + (1-2\nu_p)/E_p]\sigma_r^2}, \tag{4}$$

where γ is the surface energy of the particle, and σ_r is the radial stress.

B. Tests of theory

The measurement of residual stresses in glass matrices containing crystalline inclusions is controversial.[10] Various publications have differed in both the particle size dependence of the residual stress,[11,12] as well as its magnitude,[13,14] as compared with the predictions outlined in the previous section. A number of recent publications are related to the measurement of residual stresses in glass matrices with refractory inclusions and reinforcing particles, and at least two reports deal specifically with residual stresses in glass ceramics,[15,16] but they did not aim at testing the Selsing and Davidge and Green models.

Some of the present authors reported on experimental tests of the existing models using partially crystallized glass ceramics.[10,17] We studied a partially crystallized P_2O_5-doped soda-lime-silica bioglass that nucleates in the volume and whose microstructure was designed to yield a volume fraction crystallized below 15%.[10] The residual stresses were measured by an x-ray diffraction (XRD) technique for a special set of *hkl* planes. The experimental residual stress ($\sim$160 MPa) agreed, within experimental error, with the value calculated by the Selsing model. On the other hand the predicted critical diameter for spontaneous cracking, D_c, calculated by an energy balance approach [Eq. (4)] was about ten times smaller than the experimental diameter. These results thus suggest that the energy balance model underestimates D_c, and so particles of sizes not only less than D_c but even somewhat greater are stable against spontaneous cracking.

In a second study we calculated the level of residual stresses in partially crystallized $Li_2O-2SiO_2$ glass ceramics by the Selsing model, and also determined these stresses by an x-ray diffraction method using synchrotron radiation.[17] The linear thermal expansion coefficient of a fully crystallized, stress-free, powdered sample was measured *in situ* using a hot-stage x-ray diffraction technique. The average thermal expansion coefficient calculated from the unit cell expansion with temperature $\langle\alpha_{uc}\rangle = (10.1\pm0.5)\times10^{-6}\ K^{-1}$ was close to that obtained by a dilatometric method for a polycrystalline sample $\langle\alpha_p\rangle = (10.8\pm0.5)\times10^{-6}\ K^{-1}$. We then calculated the residual stresses using the Selsing model and experimental data for the elastic constants combined with thermal expansion coefficient data. The experimental results agreed reasonably well with the calculated magnitudes of the residual stresses. Therefore, we concluded in both studies that the Selsing model can give reasonable estimates of residual stresses in glass ceramics.

III. MATERIALS AND METHODS

A. Sample preparation

A PTR glass containing SiO_2, Na_2O, ZnO, and Al_2O_3 as the major components, K, F, and B as minor components, and about 100 ppm of each of the following dopants: Ce_2O_3, SnO, Sb_2O_3, and Ag_2O, was melted in a Pt–3%Rh crucible for about 4 h, and then stirred for an additional 2 h, all at 1460 °C in an electric furnace. The liquid was then cast on a steel plate and annealed in the range of 460–400 °C, which is near to T_g, for about 1 h. Several samples were then cut from the original glass blank for further analysis.

Polished samples were exposed to homogeneous UV irradiation at room temperature using an expanded beam of a He–Cd laser at 325 nm, with a dosage of 0.9 J cm^{-2}. Crystallization thermal treatment was in the range from 400 to 520 °C.

B. Measurements of physical properties

Overall refractive index change measurements of PTR glass after photoinduced crystallization were carried out using a shearing interferometer by a technique previously developed and described.[18] By this method a polished sample is stripe irradiated by dragging the sample across a laser beam with a known beam profile. After development, the sample is installed between two optical quartz plates and submerged into a liquid of matched refractive index. The interferometer detects the image of refractive index modulation along the irradiated stripe. After digital analysis of the interferograms photosensitometric dependence of the refractive index change on irradiation dosage (dn vs dE) can be obtained. This technique allows measurement of refractive index changes with an accuracy of 5×10^{-6}.

Young's modulus E and the Poisson ratio ν were obtained from the literature.[19] Thermal expansion measurements have been performed in a previous work.[20] XRD experiments have been described previously.[21]

C. NMR experiments

NMR spectra of PTR samples before and after heat treatment, as well as of bulk NaF powder, were acquired on a Bruker Avance NMR spectrometer operating at 16.44 T (700 MHz proton frequency). ^{23}Na and ^{19}F NMR spectra were measured under 30 kHz magic angle spinning (MAS) conditions using rotors of 2.5 mm diameter. Eighty scans were accumulated for the ^{23}Na NMR spectra of the PTR samples using 90° pulse lengths of 3.25 μs and 32 s recycle times. The ^{23}Na NMR spectra were referenced against a 0.1M aqueous NaCl solution. Similarly, 80 scans were acquired for the ^{19}F NMR spectra of the PTR samples using 90° pulse lengths of 2.4 μs and 30 s recycle times. The ^{19}F spectra were referenced against neat CF_3CO_2H at −76.55 ppm. Peak positions were determined from deconvolutions of the NMR spectra using mixed Gaussian/Lorentzian line shapes, including spinning sidebands where appropriate, in order to avoid systematic errors arising from the overlap of the signals from the glassy and crystalline phases.

Triple quantum MAS (3Q-MAS) NMR experiments were carried out on a Varian spectrometer operating at 9.4 T using a three pulse sequence with z filter.[22,23] Pulse amplitudes of 90 kHz for excitation and reconversion and 5 kHz for z filtering were used. A number of 128 hypercomplex free induction decay (FID) signals were collected, with 1024 points and 2400 transients each and a recycle delay of 1 s. Samples were spun at 7 kHz in 7 mm silicon nitride rotors. Aqueous 0.1M NaCl was used as chemical shift reference.

The relatively coarse powders used for NMR experiments (powder particle diameter greater than 20 μm) were much larger than the estimated NaF crystal sizes, hence, it can be inferred that no significant stress relaxation occurred during grinding, since the majority of the crystals remained inside the glass grains.

D. First principles calculations

Calculations of the refractive index and NMR parameters of the NaF particles were carried out with the CASTEP package.[24,25] This code implements a density functional theory (DFT) approach to electronic structure calculations on periodic solids using a plane wave basis and pseudopotentials to describe the core electrons. The present calculations were performed using the local density approximation. Although generalized gradient functionals give better results for chemical shifts when comparing many different chemical sites to experiment, here we will be comparing the relative shift of one site at different values of a mild, non-symmetry-breaking perturbation. Therefore in the interest of computational efficiency we chose to use the local density approximation.

For the NMR calculations, we used ultrasoft pseudopotentials generated from the "on-the-fly" method implemented within CASTEP. We treated the 2s, 2p, and 3s electrons of sodium explicitly in the valence space, and the 2s and 2p electrons of fluorine. We used a plane wave cutoff energy of 610 eV, and integrated over reciprocal space using a $10\times10\times10$ Monkhorst-Pack grid, which for the primitive cell used amounted to a grid spacing of 0.038 $Å^{-1}$.[26] Within this approach the optimized conventional unit cell size for NaF was found to be 4.542 Å, compared with the experimental value of 4.632 Å,[27] and the bulk modulus was computed to be 36.3±2.1 GPa, as compared with the experimental value of 46±6 GPa.[28,29]

Optical properties were computed using norm-conserving pseudopotentials. These gave levels of agreement for experimental properties similar to the ultrasoft pseudopotentials described above; the main difference was that a higher cutoff energy, 850 eV, was used. The band gap for NaF computed this way was smaller than the experimental value of about 11.4 eV. To bring the computed band gap into agreement with experiment, a scissor operator of 5 eV was employed.[30,31] This scissor operator was also used in computing the index of refraction discussed below.

Further optimization under hydrostatic pressure conditions (both tensile and compressive) was carried out as desired. For the final structures, optical and NMR properties were computed within the CASTEP package.

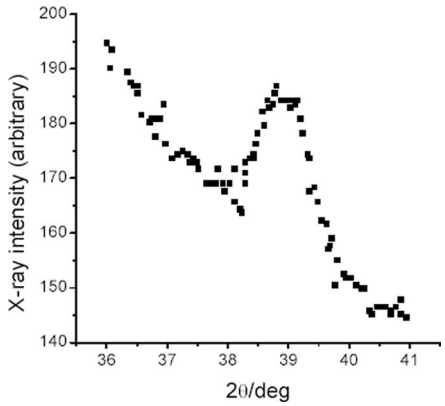

FIG. 1. Portion of XRD pattern of PTR glass after exposure to UV radiation at 325 nm for 2 J cm^{-2} and heat treatment at 520 °C for 1 h (see Ref. 21). The peak shown matches the (200) reflection of NaF.

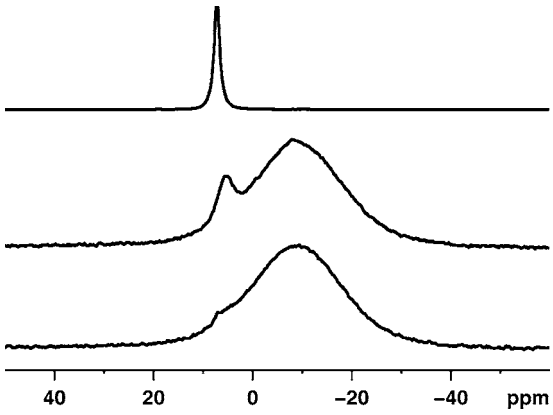

FIG. 3. ^{23}Na magic angle spinning NMR spectra of PTR glass and bulk NaF at 16.44 T. Bottom: Base PTR glass. Middle: PTR glass after ceramming treatment. Top: Bulk NaF.

IV. RESULTS

The XRD pattern reproduced in Fig. 1 and other data[21] show indications of the NaF crystalline phase after typical heat treatments for several hours between 520 and 600 °C. Typically, only one to three Bragg reflections are evident in the crystallized samples.[21] These fit the spacings of NaF.

The solid-state NMR spectra reported here provide additional strong evidence for this phase: both the ^{19}F and ^{23}Na spectra (Figs. 2 and 3) show a sharp, well resolved feature that appears as the glass is partially cerammed. The shifts for these features are listed in Table I. These features are nearly identical in shift and linewidth to those observed in bulk NaF, confirming by an element-specific technique the identification of the microcrystalline phase. The shifts between the peaks in the samples and those in bulk NaF, while small, are nevertheless significant, and will be discussed further below.

The ^{23}Na 3Q-MAS experiments carried out in the irradiated/treated sample (Fig. 4) showed the presence of two signals, the projections across the isotropic and anisotropic axes which gave the chemical shifts δ_{CS}^{iso} (in ppm) and electric quadrupole coupling parameters C_Q shown in Table II. Peak I corresponds to Na sites in the glass matrix. The moderately high value of the quadrupole coupling constant C_Q of these sites (1.3 MHz) indicates noncubic point symmetry, with a coordination number for Na between 5 and 6.[32] On the other hand, the peak corresponding to site II is correlated with the narrower peak observed in the one-dimensional (1D) MAS spectrum. The value of C_Q is indistinguishable from zero, within the uncertainty of the 3Q-MAS determination, indicating a very low electric field gradient at these sites. This result is consistent with the attribution of this peak to NaF nanocrystals, since such sites have cubic symmetry. This result also indicates that the shifts at even higher field shown in Table I can be taken to be of purely chemical shift in origin, even for ^{23}Na. A 3Q-MAS experiment carried out on a bulk polycrystalline sample of NaF gave equivalent results for C_Q, but also showed a clear deviation of the isotropic shift, as shown in Table II.

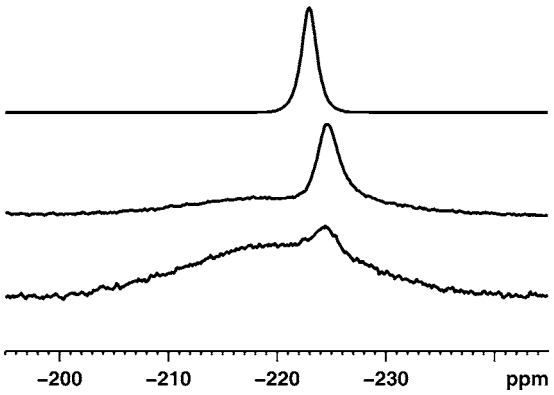

FIG. 2. ^{19}F magic angle spinning NMR spectra of PTR glass and bulk NaF at 16.44 T. Bottom: Base PTR glass. Middle: PTR glass after ceramming treatment. Top: Bulk NaF.

From published thermal expansion data for the PTR glass an average coefficient of linear thermal expansion of $\alpha_g = 8.4 \times 10^{-6}$ K^{-1} was determined for the temperature range of 25–450 °C.[20] The thermal expansion coefficient of bulk NaF in the same temperature range is $\alpha_c = 36 \times 10^{-6}$ K^{-1}.[19] The knowledge of these estimated values are sufficient for our purposes. As $\alpha_g < \alpha_c$ and the embedded crystals retain cubic symmetry, we infer that they are under an isostatic tensile stress field.

The modulus of elasticity of the base PTR glass, E, was estimated using the SCIGLASS software package to be 64 GPa, based on its approximate chemical composition, and that of NaF, 79 GPa, was obtained from the literature.[19] The Poisson ratio ν_m of the glass was taken to be approximately 0.2–0.3, typical of oxide glasses, whereas the Poisson ratio of NaF is 0.33.[19]

After partial crystallization at 520 °C, the overall refractive index difference between the UV-irradiated and nonirradiated regions of PTR glass is typically 500–1000 ppm.

TABLE I. F-19 and Na-23 shifts measured under magic angle spinning conditions at 16.44 T. F-19 is referenced against neat CF_3CO_2H at −76.55 ppm, and Na-23 against 0.1*M* NaCl at 0 ppm.

Sample	$\delta_{iso}^{F\text{-}19}$ (ppm)	$\delta_{iso}^{Na\text{-}23}$ (ppm)
NaF powder	−223.00±0.01	7.25±0.01
Glass ceramic	−224.75±0.01	5.65±0.01
Base glass	−224.60±0.03	6.53±0.01

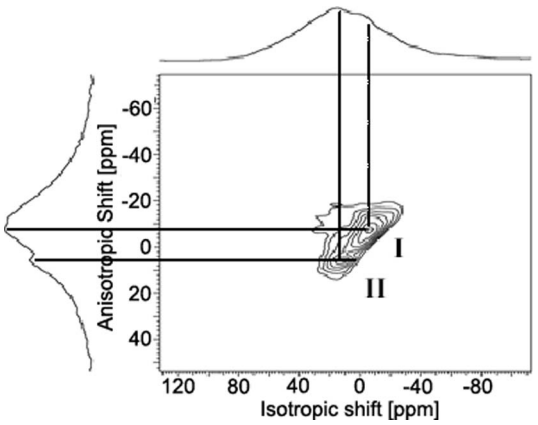

FIG. 4. ^{23}Na 3Q-MAS spectrum in the irradiated and heated sample. Peak I: Na sites in glass matrix. Peak II: Na sites in NaF nanocrystals.

V. DISCUSSION: RESIDUAL STRESS IN PTR GLASS

The stresses at the particle/matrix interface were calculated by Eqs. (1) and (2) and the Selsing formula, Eq. (3). The following data were used: $\Delta\alpha = 27.6 \times 10^{-6}\ \mathrm{K}^{-1}$, $\Delta T = 440\ ^\circ\mathrm{C}$ (we consider a temperature range in which the matrix plasticity is negligible, from T_g to room temperature), $\nu_m = 0.20$, $\nu_p = 0.33$, $E_m = 64$ GPa, and $E_p = 79$ GPa. By substituting these values into Eq. (3), the calculated σ_r is about 680 MPa (tensile). If we use an upper bound for the glass Poisson ratio, i.e., 0.30, the calculated residual stress value drops to 650 MPa.

Searching for evidence of this stress directly in the x-ray pattern (Fig. 1) is complicated by the small particle size. In contrast, NMR is not dependent on crystallite size effects, and so can detect features in nanomaterials that are unclear in x-ray scattering. Careful analysis of the shifts of the NMR spectra shown in Figs. 2 and 3 compared with bulk NaF, permits an alternative determination of the residual stress. By optimizing the computed structure of NaF under hydrostatic pressure conditions ranging from 2 GPa (tensile) to 2 GPa (compressive) and computing the ^{19}F and ^{23}Na chemical shifts, we computed the shifts shown in Fig. 5. These results showed small but distinct curvature and were fit by functions of the form $\delta(P) = aP^2 + mP + b$, where P is pressure, and a, m, and b are free fit parameters. We found for ^{19}F

$$\begin{aligned}\delta_{\mathrm{iso}} = {} & P^2(-0.080 \pm 0.008)\ \mathrm{ppm\ GPa^{-2}} \\ & + P(2.035 \pm 0.010)\ \mathrm{ppm\ GPa^{-1}} \\ & + (-0.072 \pm 0.015)\ \mathrm{ppm}, \end{aligned} \tag{5}$$

and for ^{23}Na,

TABLE II. Positions of ^{23}Na 3Q-MAS projected peaks and calculated coupling parameters for the observed signals in irradiated PTR glass and in bulk polycrystalline NaF.

Sample/peak	δ_{iso} (ppm)	δ_{aniso} (ppm)	$\delta_{\mathrm{CS}}^{\mathrm{iso}}$ (ppm)	C_Q (MHz)
Irradiated/I	−5.6±0.3	−8.5±0.2	4.8±0.2	1.3±0.1
Irradiated/II	13.0±0.5	5.5±0.3	6.0±0.4	0.0±0.5
NaF powder	14.5±0.2	7.0±0.2	6.9±0.1	0.0±0.2

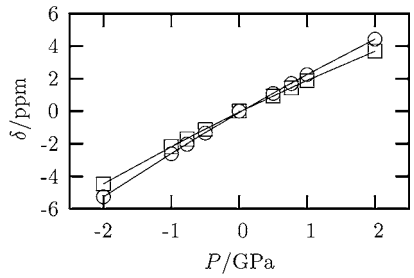

FIG. 5. Computed chemical shifts for ^{23}Na (circles) and ^{19}F (squares) in NaF as a function of hydrostatic pressure. Solid lines are quadratic fits of the form $\delta(P) = aP^2 + mP + b$, where P is pressure, and a, m, and b are free fit parameters. Shifts are referenced to the computed shift for NaF at zero pressure.

$$\begin{aligned}\delta_{\mathrm{iso}} = {} & P^2(-0.080 \pm 0.01)\ \mathrm{ppm\ GPa^{-2}} \\ & + (2.423 \pm 0.013)\ \mathrm{ppm\ GPa^{-1}} \\ & + (-0.092 \pm 0.019)\ \mathrm{ppm}. \end{aligned} \tag{6}$$

The errors stated here are those derived from the fitting procedure. Experimentally, we observed shifts in the ^{19}F and ^{23}Na spectra relative to bulk NaF of −1.75 and −1.60 ppm, respectively (Table I), leading to estimates of the pressure as 800 MPa (tensile) and 610 MPa (tensile). These derived estimates for the stress are in good agreement with that from the Selsing model.

Assuming a typical value for the fracture energy of silicate glasses, $\gamma = 3.5\ \mathrm{J\ m^{-2}}$, the calculated critical diameters from Eq. (4) for spontaneous fracture are 2300–1900 nm for 680 and 800 MPa, respectively. These greatly exceed the observed crystal particle diameters of 7–35 nm, thus no spontaneous fracture is expected in partially crystallized PTR glass.

The dependence of the optical refractive index on pressure for the NaF particles is estimated from our first principles calculations to be very weak. For NaF at zero pressure we compute an optical index of refraction of 1.316, while under 700 MPa hydrostatic stress (tensile) this value drops to 1.315, a change of only −0.08%. Further studies are needed to reveal if these changes in refractive index are significant for the optical properties of PTR glass gratings.

VI. CONCLUSIONS

The residual internal stresses around the NaF crystals in PTR glass calculated by the Selsing model are approximately 680 MPa tensile while the values determined by NMR coupled with DFT simulations are 610–800 MPa tensile. In this study NMR has been used for residual stress determination in a bulk composite and the observed agreement confirms the validity of the Selsing model. The calculated critical diameter for spontaneous cracking greatly exceeds the observed NaF crystal diameters. Thus self-cracking is not expected in PTR glass.

DFT calculations show that these stresses have only a small effect on the refractive index of the precipitated NaF crystals. Such small changes are confirmed by measurements of the overall changes in the PTR glass refractive index after partial crystallization.

ACKNOWLEDGMENTS

We thank the Canada Foundation for Innovation, the Natural Sciences and Engineering Research Council of Canada, and the Canada Research Chairs program for financial support. The financial help of CNPq and Capes (Brazil), and of CIAM-CNPq/NSERC (Inter-American collaboration on materials) are fully appreciated. We thank Dr. M. L. F. Nascimento of LaMaV/UFSCar (Brazil) for calculations with the SCIGLASS software.

[1]G. Partridge, Glass Technol. **35**, 116 (1994).
[2]D. W. Jones, Key Eng. Mater. **122**, 345 (1996).
[3]W. Pannhorst, in *Low Thermal Expansion Glass Ceramics*, edited by H. Bach (Springer, Berlin, 1995), pp. 107–214.
[4]J. Selsing, J. Am. Ceram. Soc. **44**, 419 (1961).
[5]B. Q. Li and Y. N. Wang, J. Appl. Phys. **75**, 1783 (1993).
[6]J. S. Lord, H. Kubo, P. C. Riedi, and M. J. Walker, J. Appl. Phys. **73**, 6381 (1993).
[7]T. Thomson, P. C. Riedi, K. P. Wellock, and B. J. Hickey, J. Appl. Phys. **81**, 4469 (1997).
[8]T. M. Alam, T. A. Friedmann, P. A. Schultz, and D. Sebastiani, Phys. Rev. B **67**, 245309 (2003).
[9]R. W. Davidge and T. J. Green, J. Mater. Sci. **3**, 629 (1968).
[10]V. R. Mastelaro and E. D. Zanotto, J. Non-Cryst. Solids **194**, 297 (1996).
[11]R. M. Fulrath, J. Am. Ceram. Soc. **42**, 423 (1959).
[12]L. A. Zevin, E. A. Levy, and Z. G. Bessmertnaya, Izv. Akad. Nauk SSSR, Neorg. Mater. **13**, 1880 (1977).
[13]M. P. Borom, A. M. Turkalo, and R. H. Doremus, J. Am. Ceram. Soc. **58**, 385 (1975).
[14]N. Miyata, K. Tanigawa, and H. Jinno, in *Fracture Mechanics of Ceramics*, edited by R. C. Bradt, P. P. H. Hasselman, and F. Lange (Plenum, New York, 1983), Vol. 5, p. 609.
[15]S. Widjaja, Mater. Charact. **47**, 47 (2001).
[16]P. C. Soares, Jr. and C. M. Lepienski, J. Non-Cryst. Solids **348**, 139 (2004).
[17]V. R. Mastelaro and E. D. Zanotto, J. Non-Cryst. Solids **247**, 79 (1999).
[18]O. M. Efimov, L. B. Glebov, L. N. Glebova, K. C. Richardson, and V. I. Smirnov, Appl. Opt. **38**, 619 (1999).
[19]Crystran Ltd., NaF Data Sheet, URL: http://www.crystran.co.uk/nafdata.htm
[20]H. François-St.-Cyr, Ph.D. thesis, University of Central Florida, 2001.
[21]T. Cardinal O. M. Efimov, H. G. Francois-St.-Cyr, L. B. Glebov, L. N. Glebova, and V. I. Smirnov, J. Non-Cryst. Solids **325**, 275 (2003).
[22]D. Massiot B. Touzo, D. Trumeau. J. P. Coutures, J. Virlet, P. Florian, and P. J. Grandinetti, Solid State Nucl. Magn. Reson. **6**, 73 (1996).
[23]J.-P. Amoreaux, C. Fernandez, and S. Steuernagel, J. Magn. Reson., Ser. A **123**, 116 (1996).
[24]M. D. Segall P. J. D. Lindan, M. J. Probert, C. J. Pickard, P. J. Hasnip, S. J. Clark, and M. C. Payne, J. Phys.: Condens. Matter **14**, 2717 (2002).
[25]C. J. Pickard and F. Mauri, Phys. Rev. B **63**, 245101 (2001).
[26]H. J. Monkhorst and J. D. Pack, Phys. Rev. B **13**, 5188 (1976).
[27]R. B. Srinivasa and S. P. Sanyal, Phys. Rev. B **42**, 1810 (1990).
[28]R. L. Erikson, L. E. Eary, and C. J. Hostetler, J. Chem. Phys. **99**, 336 (1992).
[29]Y. Sato-Sorensen, J. Geophys. Res. **88**, 3543 (1983).
[30]Z. H. Levine and D. C. Allan, Phys. Rev. Lett. **63**, 1719 (1989).
[31]X. C. Gonze and C. Lee, Phys. Rev. B **55**, 10355 (1997).
[32]H. Koller, G. Engelhardt, A. P. M. Kentgens, and J. Sauer, J. Phys. Chem. **98**, 1544 (1994).